Ada W.C.Yan, Andrew J.Black, James M.McCaw, Nicolas Rebuli, Joshua V.Ross, Annalisa J.Swan, Roslyn I.Hickson

The distribution of the time taken for an epidemic to spread between two communities

Mathematical Biosciences, 2018; 303:139-147

The distribution of the time taken for an epidemic to spread between two communities

Ada W. C. Yan[a,b], Andrew J. Black[c], James M. McCaw[b,d,e], Nicolas Rebuli[c], Joshua V. Ross[c], Annalisa J. Swan[a], Roslyn I. Hickson[a,*]

[a] *IBM Research – Australia, Melbourne, VIC 3006, Australia*
[b] *School of Mathematics and Statistics, University of Melbourne, Parkville, VIC 3010, Australia*
[c] *School of Mathematical Sciences, The University of Adelaide, Adelaide, SA 5005, Australia*
[d] *Centre for Epidemiology and Biostatistics, Melbourne School of Population and Global Health, University of Melbourne, Parkville, VIC 3010, Australia*
[e] *Modelling and Simulation, Infection and Immunity Theme, Murdoch Childrens Research Institute, Parkville, VIC 3052, Australia*

Abstract

Assessing the risk of disease spread between communities is important in our highly connected modern world. However, the impact of disease- and population-specific factors on the time taken for an epidemic to spread between communities, as well as the impact of stochastic disease dynamics on this spreading time, are not well understood. In this study, we model the spread of an acute infection between two communities ('patches') using a susceptible-infectious-removed (SIR) metapopulation model. We develop approximations to efficiently evaluate the probability of a major outbreak in a second patch given disease introduction in a source patch, and the distribution of the time taken for this to occur. We use these approximations to assess how interventions, which either control disease spread within a patch or decrease the travel rate between patches, change the spreading probability and median spreading time.

We find that decreasing the basic reproduction number in the source patch is the most effective way of both decreasing the spreading probability, and delaying epidemic spread to the second patch should this occur. Moreover, we show that the qualitative effects of interventions are the same regardless of the approximations used to evaluate the spreading time distribution, but for some regions in parameter space, quantitative findings depend upon the approximations used. Importantly, if we neglect the possibility that an intervention prevents a large outbreak in the source patch altogether, then intervention effectiveness is not estimated accurately.

Keywords: disease spread, metapopulation, branching process, extinction probability, arrival time

*Corresponding author
Email address: R.Hickson@UNSWalumni.com (Roslyn I. Hickson)

1. Introduction

Infectious disease spread across regions has become more rapid due to increased global mobility (Cliff et al., 2009). Understanding how disease- and population-specific factors influence the timing of disease importation is important for effective interventions to prevent or delay disease spread.

As reviewed by Arino (2017), metapopulation models are useful for modelling the spread of disease between regions, or 'patches', where within-patch disease transmission occurs more frequently than between-patch transmission (Rvachev & Longini, 1985). In this study, we focus on the early stages of the epidemic, when it first begins to spread from its source patch. Previous studies of metapopulation models have used branching process approximations to calculate outbreak probabilities (Ball et al., 1997; Lahodny & Allen, 2013). However, these studies do not examine the timing of disease spread. Studies which address the timing of travel of infectious individuals, and thus of disease spread, have assumed deterministic within-patch disease dynamics (Gautreau et al., 2008; Barthélemy et al., 2010; Wang & Wu, 2018). The studies also do not explicitly include the effect of interventions. Importantly, all of these studies assume that travel results in permanent migration, but short-term travel may be a greater driving force in the spread of infection (Keeling & Rohani, 2002). Threshold conditions for outbreaks assuming short-term travel have been previously determined (Balcan & Vespignani, 2012), but the temporal dynamics of such models were not analysed.

In this study, using a two-patch susceptible-infectious-removed (SIR) model with stochastic disease dynamics and short-term travel between patches, we analyse the temporal aspect of disease spread, addressing limitations of previous studies. We evaluate the distribution of the time taken for the epidemic to spread to the second patch (the *spreading time distribution*), and the probability that such spread occurs (the *spreading probability*). In Section 2, we outline the methods used to perform these calculations. We proceed to explore how interventions change the spreading probability and median spreading time (Section 3.1), and how approximations can be made to calculate the spreading time distribution accurately and efficiently (Section 3.2).

2. Methods

In Section 2.1, we specify the 'ground truth' model for this study. However, exact calculation of the spreading time distribution for this model is computationally infeasible. Therefore, in Section 2.2.1 we make approximations to simplify the model, before deriving an expression for the spreading time distribution in Sections 2.2.2–2.2.3. Three methods for evaluating the spreading time distribution for the reduced model, with varying degrees of approximation, are presented in Section 2.3. In Section 3, we will use these three methods to

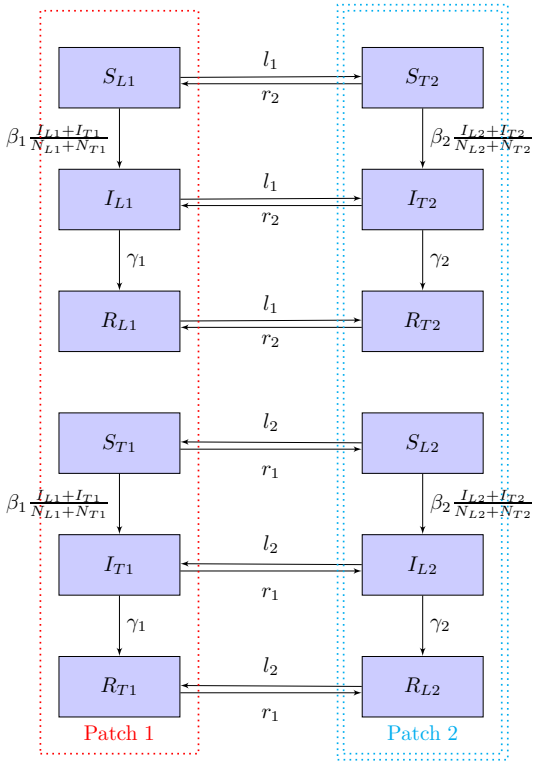

Figure 1: *The 'ground truth' model.* The red dotted rectangle and cyan dotted double rectangle indicate the extent of Patch 1 and Patch 2 respectively. The subscripts 1 and 2 denote the current location of the individual, and the subscripts L and T denote whether they are local to that patch or a traveller. Table 1 defines the model parameters.

obtain the spreading time distribution, and compare them with the spreading time distribution obtained by simulating from the 'ground truth' model.

2.1. The model

Figure 1 illustrates the 'ground truth' model for this study: a two-patch SIR model where within-patch disease dynamics and movement between patches are modelled stochastically. The formal specification of the model as a continuous-time Markov chain (CTMC) $\{\mathbf{X}(t)\}$ is given in Appendix A.

Table 1 defines the model parameters. Within each patch i, susceptibles S_{Li}, S_{Ti} are infected by infectious individuals I_{Li}, I_{Ti} at a rate β_i. The subscripts Li and Ti denote locals to patch i and travellers temporarily in patch i respectively. Infectious individuals then recover at a rate γ_i. The leaving rate per local in home patch i is given by l_i, and the return rate per traveller currently in patch i is given by r_i. The basic reproduction number in each patch, conditioned on no travel, is given by

Parameter	Description	Default value
β_i	Transmission parameter in patch i	calculated according to R_{0i}
γ_i	Recovery rate in patch i	1
R_{0i}	Basic reproduction number in patch i	5
l_i	Rate at which locals of patch i leave patch i	10^{-2}
r_i	Rate at which travellers in patch i leave patch i	1
$N_{Li}(0)$	Initial number of locals in patch i	$N_{L1}(0) + N_{T1}(0) = N_{L2}(0) + N_{T2}(0) = 500$
$N_{Ti}(0)$	Initial number of travellers in patch i	see Eq. 2
ϕ_{Li}	Probability that one infectious local causes an outbreak in patch i	derived in Section 2.2.3
ϕ_{Ti}	Probability that one infectious traveller causes an outbreak in patch i	derived in Section 2.2.3
κ_L	Rate at which infectious locals in Patch 1 travel to Patch 2 and cause an outbreak	defined in Eq. (3)
κ_T	Rate at which infectious travellers in Patch 1 return to Patch 2 and cause an outbreak	defined in Eq. (3)

Table 1: *Parameters and derived quantities.* Note that all rates are scaled such that $\gamma_i = 1$, and are hence in units of (mean infectious period)$^{-1}$. To specify $N_{Li}(0)$ and $N_{Ti}(0)$, $N_{Li}(0) + N_{Ti}(0)$ is fixed, and their ratio calculated using Eq. 2.

$$R_{0i} = \frac{\beta_i}{\gamma_i}. \tag{1}$$

All references to R_{0i} in the study refer to this quantity.

We assume that population sizes are at equilibrium initially, such that

$$N_{T2}(0) = \frac{l_1}{r_2} N_{L2}(0), \tag{2}$$

and similarly for $N_{T1}(0)$. For example, for the values in Table 1, $N_{T2}(0) = N_{L2}(0)/100$; combined with the population size $N_{L2}(0) + N_{T2}(0) = 500$, we obtain $N_{L2}(0) = 495.05$, $N_{T2}(0) = 4.95$, which we round to $N_{L2}(0) = 495$, $N_{T2}(0) = 5$. We assume that the epidemic starts with one infectious local in Patch 1. Calculations can be adjusted for the case where the epidemic starts instead with one infectious traveller, or with more than one infectious individual (not shown).

2.2. Calculating the spreading time distribution

We define the *spreading time* as the time at which an infectious individual who proceeds to cause a major outbreak in Patch 2 arrives in that patch. The *spreading probability* is the probability that such an event occurs. A *major outbreak* is informally defined as one where a significant proportion of the population is infected. For the 'ground truth' model, we define a major outbreak as

having a transmission chain in Patch 2 whose final size exceeds 10 individuals (out of $N_2 = 500$ individuals in the patch). For some parameter values, the spreading time distribution is sensitive to the value chosen for this threshold; the difficulties thus arising are discussed in Section 2.1 of the Supplementary Material.

Two possible events trigger a major outbreak to occur in Patch 2, as previously considered by Lopez et al. (2016) (in a deterministic context): either

- an infectious individual from Patch 1 travels to Patch 2 and starts a major outbreak; or
- a susceptible individual from Patch 2 travels to Patch 1, contracts the disease, returns, and starts a major outbreak.

2.2.1. Reducing the 'ground truth' model

In theory, the spreading time distribution can be numerically evaluated. This would be achieved by numerical solution of the forward equation of the continuous-time Markov chain (see Jenkinson & Goutsias (2012). for one approach), to provide the probability distribution of the number of infectious individuals in Patch 2 at any given time, and a choice of threshold above which a major outbreak is declared. Unfortunately, such an approach is computationally infeasible for all but the smallest population sizes, as the size of the state space is $\mathcal{O}(N_1^6 N_2^6)$. This means that even estimation of the spreading time distribution can be computationally expensive. Hence, we reduce the 'ground truth' model by assuming that up until the spreading time:

- susceptibles are not depleted in Patch 2 (S_{L2} and S_{T2} are constant);
- the movement of individuals changes the population size in each patch negligibly (N_{Li} and N_{Ti} are constant);
- changes in numbers of susceptible and recovered locals and travellers in each patch are driven by infection rather than travel, such that travel of susceptible and recovered individuals can be ignored; and
- the travel rates l_i are sufficiently small compared to the recovery rates γ_i, such that the disease dynamics in Patch 1 are driven by transmission within that patch and not by importation of infectious individuals.

The validity of the last assumption depends both on the timescale of the movement between patches and the recovery time of the disease modelled. For example, the assumption may not hold if daily commuting is a significant contributor to travel.

The first assumption allows us to approximate disease dynamics in Patch 2 as a branching process, which we will define in Section 2.2.3 (see Harris (1963) for the theory of branching processes, Kimmel & Axelrod (2015) for branching processes in biology, and Ball (1983) for modelling the initial stages of an epidemic as a branching process). Instead of defining a major outbreak according

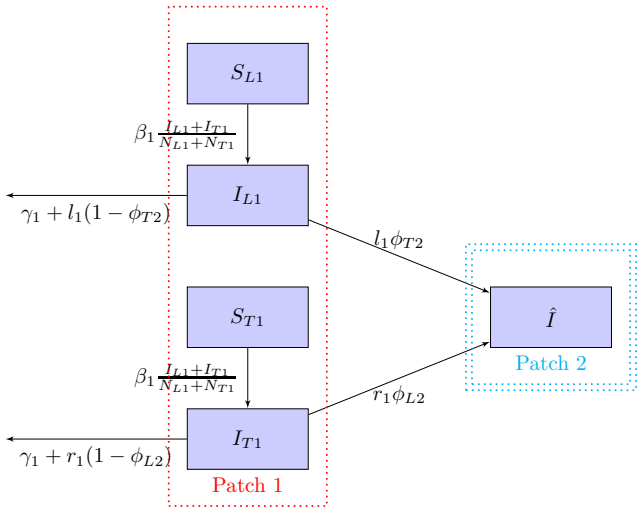

Figure 2: *The reduced model.* The subscripts L and T denote whether an individual is local to Patch 1 or a traveller. $\hat{I}$ counts the individuals in Patch 2 who lead to an unbroken transmission chain in that patch. Table 1 defines the model parameters.

to a threshold, we use the branching process non-extinction probability as the spreading probability.

Under the above assumptions, the model can be reduced to a CTMC $\{\mathbf{Y}(t)\}$ given in Appendix A and illustrated in Fig. 2. $\hat{I}$ counts the individuals in Patch 2 who lead to an unbroken transmission chain in that patch. ϕ_{L2} and ϕ_{T2} are the probabilities that one infectious local/traveller in Patch 2 causes a major outbreak respectively. We will derive expressions for these quantities in Section 2.2.3.

2.2.2. Deriving expressions for the spreading time distribution

As the size of the state space of the reduced model CTMC is $\mathcal{O}(N_1^2 N_2^2)$, for population sizes of interest herein it is not feasible to numerically solve the forward equation for the spreading time distribution. Instead, we simulate a number of paired realisations of $I_{L1}(t)$, $I_{T1}(t)$; evaluate the spreading time distributions conditioning on each trajectory pair; and take the mean of those distributions to obtain our final estimate of the spreading time distribution. Bootstrapping is used to quantify the uncertainty in our estimate.

We define

$$\kappa_L := l_1\phi_{T2}, \tag{3a}$$

$$\kappa_T := r_1\phi_{L2} \tag{3b}$$

to be the rates at which infectious locals $I_{L1}(t)$ and travellers $I_{T1}(t)$ from Patch 1 cause a major outbreak in Patch 2 respectively. Then the arrival of outbreak-causing individuals in Patch 2 is a non-homogeneneous Poisson process with an intensity $\kappa_L I_{L1}(t) + \kappa_T I_{T1}(t)$. Wang & Wu (2018) used a similar

non-homogeneneous Poisson process for a model assuming permanent migration. However, the aforementioned study assumed that all infectious individuals arriving in Patch 2 cause a major outbreak. In our study, we explicitly incorporate the probability that an infectious individual arriving in Patch 2 causes an outbreak, through the probabilities ϕ_{L2} and ϕ_{T2}. Because temporary travellers spend less time than locals in Patch 2, they are (per capita) less likely to cause an outbreak; thus, the two probabilities are different.

The probability that no outbreak-causing infectious individuals have arrived in Patch 2 by time t is given by

$$p(\hat{I} = 0, t) = \exp(-\mu(t)) \tag{4a}$$

$$\text{where} \qquad \mu(t) = \int_0^t \kappa_L I_{L1}(\tau) + \kappa_T I_{T1}(\tau) d\tau. \tag{4b}$$

Hence, for given trajectories $I_{L1}(t), I_{T1}(t)$, the cumulative distribution function of the arrival time (spreading time) is given by

$$p(T_{spread} < t) = 1 - p(\hat{I} = 0, t) = 1 - \exp[-\mu(t)], \tag{5}$$

the probability density function for the spreading time is given by

$$p(T_{spread} = t) = -\frac{d}{dt} p(X = 0, t) = \exp[-\mu(t)] \frac{d}{dt} \mu(t), \tag{6}$$

and the spreading probability is given by

$$p(T_{spread} < \infty) = \lim_{t \to \infty} 1 - \exp[-\mu(t)]. \tag{7}$$

Importantly, the spreading time distribution conditioning on particular trajectories $I_{L1}(t), I_{T1}(t)$ is a function only of the composite parameters κ_L, κ_T. Note that the probability density function is improper, with its integral being the spreading probability.

2.2.3. Deriving expressions for the spreading probability per import, ϕ_{L2} and ϕ_{T2}

We model disease dynamics in Patch 2 using the time-homogeneous CTMC $\{\mathbf{Z}(t)\}_{t \geq 0}$ which takes values (I_{L2}, I_{T2}) where $I_{L2}, I_{T2} \geq 0$. This CTMC is a branching process. Let $\mathbf{c}_j$ denote the stochiometries of $\{\mathbf{Z}(t)\}$ and $q_Z(\mathbf{z}, \mathbf{z} + \mathbf{c}_j)$ denote the transition rate from $\mathbf{z}$ to $\mathbf{z} + \mathbf{c}_j$, for $j = 1, \ldots, 4$. The values of $\mathbf{c}_j$ and $q_Z(\mathbf{z}, \mathbf{z} + \mathbf{c}_j)$ are given in Table 2. We define $p_{\mathbf{z} \to \mathbf{z} + \mathbf{c}_j} := q_Z(\mathbf{z}, \mathbf{z} + \mathbf{c}_j) / \sum_j q_Z(\mathbf{z}, \mathbf{z} + \mathbf{c}_j)$. The offspring generating functions are then given by

$$f_1(y_1, y_2) = p_{(1,0) \to (2,0)} y_1^2 + p_{(1,0) \to (1,1)} y_1 y_2 + p_{(1,0) \to (0,0)}, \tag{8a}$$

$$f_2(y_1, y_2) = p_{(0,1) \to (0,2)} y_2^2 + p_{(0,1) \to (1,1)} y_1 y_2 + p_{(0,1) \to (0,0)}. \tag{8b}$$

The extinction probability is the minimal non-negative solution to

j	$\mathbf{c}_j$	$q_Z(\mathbf{z}, \mathbf{z}+\mathbf{c}_j)$	Description
1	$(1,0)$	$\frac{\beta_2 S_{L2}(I_{L2}+I_{T2})}{N_{L2}+N_{T2}}$	Local becomes infected
2	$(0,1)$	$\frac{\beta_2 S_{T2}(I_{L2}+I_{T2})}{N_{L2}+N_{T2}}$	Traveller becomes infected
3	$(-1,0)$	$(\gamma_2+l_2)I_{L2}$	Local recovers/travels
4	$(0,-1)$	$(\gamma_2+r_2)I_{T2}$	Traveller recovers/travels

Table 2: *Stoichiometries and transition rates of the CTMC* $\{\mathbf{Z}(t)\} = (I_{L2}, I_{T2})$.

$$\mathbf{y} = \mathbf{f}(\mathbf{y}). \tag{9}$$

Hence, $\phi_{L2} = 1 - y_1$ is the spreading probability per infectious local in Patch 2, and $\phi_{T2} = 1 - y_2$ is the spreading probability per infectious traveller in Patch 2. We solve Eq. (9) for ϕ_{T2} and ϕ_{L2} numerically using the *fsolve* function in Octave 4.0.0 (Eaton et al., 2015). Note that if movements were assumed to be permanent, setting $r_1 = r_2 = 0$ yields $\kappa_L = l_1(1 - 1/R_{02})$ and $\kappa_R = 0$, in agreement with previous results (Wang & Wu, 2018).

2.3. Methods for obtaining disease trajectories in Patch 1

In this section, we will outline three methods for obtaining the trajectories $I_{L1}(t)$, $I_{T1}(t)$:

1. using a deterministic approximation (Section 2.3.1),
   (a) without scaling to account for the possibility that the epidemic may not become established in Patch 1, or
   (b) with this scaling;
2. using a hybrid approximation (Section 2.3.2); and
3. direct simulation (Section 2.3.3).

2.3.1. Deterministic approximation

Kurtz (1970, 1971) and Barbour (1974) show that when the number of individuals in each compartment is sufficiently large, a certain class of CTMCs (to which our models belong) can be approximated deterministically by a set of ordinary differential equations. Taking the fluid limit approximation of $\{\mathbf{Y}(t)\}$ yields a set of differential equations, where s and i are the proportion of susceptible and infectious individuals in Patch 1 respectively:

$$\frac{ds_L}{dt} = -\beta_1 s_L(i_L + i_T), \tag{10a}$$

$$\frac{di_L}{dt} = \beta_1 s_L(i_L + i_T) - (\gamma_1 + l_1)i_L, \tag{10b}$$

$$\frac{ds_T}{dt} = -\beta_1 s_T(i_L + i_T), \tag{10c}$$

$$\frac{di_T}{dt} = \beta_1 s_T(i_L + i_T) - (\gamma_1 + r_1)i_T. \tag{10d}$$

We integrate forward to obtain the trajectories $i_L(t), i_T(t)$, and translate this back into the number of infectious individuals $I_{L1}(t), I_{T1}(t)$. Barthélemy et al. (2010) uses this approach for a model with permanent migration. Gautreau et al. (2008) and Wang & Wu (2018) make the additional assumption that epidemic spread ocurs while the epidemic in Patch 1 is still exponentially growing. This assumption can be relaxed in our work.

Gautreau et al. (2008) and Barthélemy et al. (2010) assume that the epidemic becomes established in Patch 1 (that is, the final size in Patch 1 is large). This assumption can also be relaxed in our work. If the epidemic does not become established in Patch 1, the probability that an infectious individual travels to Patch 2 is greatly reduced. We can account for this reduction by scaling Eqs. (5–7) by the factor ϕ_{L1} — the probability that one infectious local in Patch 1 causes a major outbreak. For example, the spreading probability in Eq. (7) becomes

$$p(T_{spread} < \infty) = \phi_{L1} \left\{ 1 - \exp\left[- \int_0^\infty (\kappa_L I_{L1}(\tau) + \kappa_T I_{T1}(\tau)) d\tau \right] \right\}. \quad (11)$$

The probability ϕ_{L1} is calculated using versions of Eqs. (8) and (9) where for the rates in Table 2, the subscript '2' is replaced with '1'. An interpretation of the scaling is that if the epidemic does not become established in Patch 1, either no travel of infectious individuals occurs, or travel does not cause a major outbreak in Patch 2.

2.3.2. Hybrid simulations

Approximating the CTMC by ordinary differential equations requires the number of individuals in each compartment to be sufficiently large, which is not true at the start or the end of the epidemic. Hybrid Markov chain models are designed to overcome this difficulty (Rebuli et al., 2016; Ballard et al., 2016). We use a hybrid model modified from Rebuli et al. (2016) to track the numbers of locals and travellers. When the numbers of susceptible and infectious individuals $S_{L1} + S_{T1}$ and $I_{L1} + I_{T1}$ both exceed a threshold, deterministic disease dynamics are used (Eq. (10)); otherwise, the CTMC $\{\mathbf{Y}(t)\}$ is simulated. In our implementation, the threshold is chosen to be 4 individuals. Using a higher threshold does not change qualitative results (not shown).

2.3.3. Stochastic simulation

We simulate $\{\mathbf{Y}(t)\}$ using the direct algorithm popularised by Gillespie (1977). This method provides the baseline accuracy of the branching process approximation.

3. Results

This section focuses on the effect of interventions — reducing R_0 (Eq. (1)) and the travel rate l in each patch — on the spreading time distribution (Section 3.1). We will additionally investigate the effect of the approximations used (Section 3.2). All results are obtained using Octave 4.0.0 (Eaton et al., 2015), with plots made using MATLAB (2015).

3.1. The effect of interventions

First, we explore the effect of changing R_0 in each patch on the spreading time distribution (Fig. 3). R_0 is varied between 1.1 and 5, encompassing a range of pathogens for which routine childhood immunization is not available, such as Ebola, influenza and SARS. Values for the other parameters are given in Table 1. Throughout this section, the spreading time distribution is calculated using approximation (1b) as enumerated in Section 2.3: the branching process approximation, and deterministic disease dynamics in Patch 1 with scaling. Approximation (1b) was chosen because the results are more intuitively explained, while retaining accuracy and computational efficiency; however, we could have chosen any of the approximations, as the qualitative effects of interventions are the same regardless of the approximations used, as shown in the Supplementary Material.

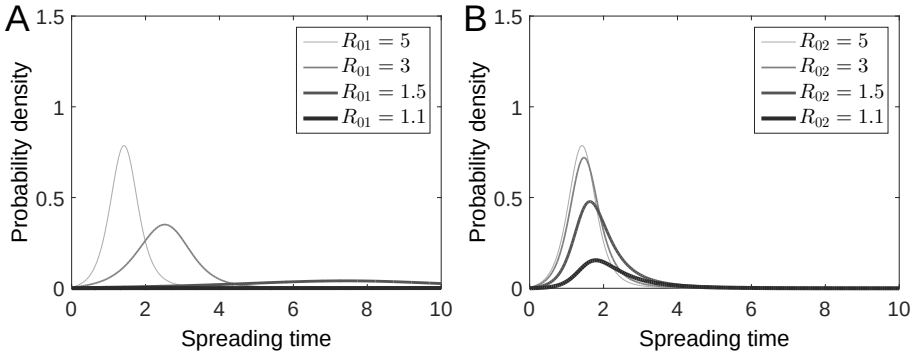

Figure 3: *Reducing R_{01} is more effective than reducing R_{02} for preventing or delaying disease spread.* The spreading time distribution for decreasing values of (a) R_{01} (b) R_{02}, calculated using approximation (1b) in Section 2.3. All other parameter values are as per Table 1. As noted in Section 2.2.2, the distributions are improper; the area under the curve represents the spreading probability.

Fig. 3A shows that as R_{01} is reduced, the spreading probability (the area under the curve) decreases. In addition, the spreading time is delayed (the distribution shifts to the right). On the other hand, as R_{02} is reduced, the spreading probability does not decrease as dramatically; the delay in the spreading time is also less apparent, making this intervention less effective than reducing R_{01}. Note that if R_0 decreases to below one in either patch, the spreading probability becomes very small and cannot be seen on the scale of the figure.

Reducing R_{01} reduces the spreading probability more because it has the potential to prevent a major outbreak in Patch 1 altogether. On the other hand, reducing R_{02} only decreases the spreading probability per import, which is incorporated in the terms κ_L and κ_T as defined in Eq. (3). Eq. (11) showed that the spreading probability is linear with respect to the outbreak probability in Patch 1 (ϕ_{L1}), but has a negative exponential relationship with κ_L and κ_T. Decreasing R_{01} also has a greater effect on the median spreading time compared

to decreasing R_{02}, because reducing R_{01} slows down the exponential growth of infectious individuals in Patch 1, slowing down importations linearly. On the other hand, decreasing R_{02} only decreases the outbreak probability per import.

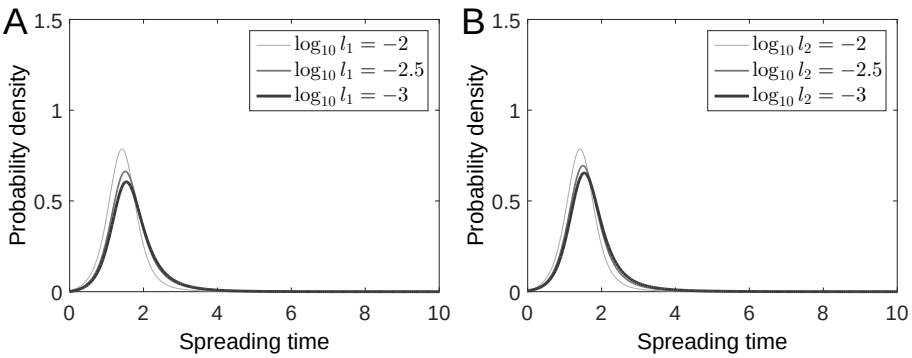

Figure 4: *Reducing l_1 and l_2 are equally ineffective at preventing or delaying an outbreak in Patch 2.* The spreading time distribution for decreasing values of (a) l_1 (b) l_2, calculated using approximation (1b) in Section 2.3. All other parameter values are as per Table 1. The distributions are improper; the area under the curve represents the spreading probability.

Figure 4 shows that reducing either l_1 or l_2 decreases the spreading probability as well as prolonging the median spreading time. However, these interventions are not as effective as reducing R_{01} (Fig. 3A). The baseline value is $l_i = 10^{-2}$, satisfying $l_i \ll \gamma_i$ as assumed in Section 2.2. As the return rate is the same as the recovery rate, at equilibrium 1% of individuals in each patch are travellers. Although we have modelled travel restriction as decreasing travel rates by tenfold at most, increasing the range of travel rates does not change qualitative results (not shown). Like reducing R_{02}, the main effect of reducing the travel rates is to decrease the terms κ_L and κ_T.

To more systematically explore parameter space, we plot the spreading probability and the median spreading time conditioning on this occurring, as either R_{01} and R_{02} are changed simultaneously, or l_1 and l_2 are changed simultaneously. (For small values of l_i, the initial condition is rounded such that there is at least one initial traveller in each patch.) Figure 5 shows that for a wide range of parameter values, decreasing R_0 or l in either patch decreases the spreading probability and delays the median spreading time; however, decreasing R_0 in the source patch is the most effective intervention in this regard.

3.2. Comparing computation methods

The previous conclusions were drawn using the branching process approximation with deterministic disease dynamics in Patch 1. This approximation not only enables analytic insight, but increases computational efficiency. Figure 6 shows the computing time using different degrees of approximation and for different population sizes, as enumerated in Section 2.3, and for the 'ground truth' model (Fig. 1 and Eq. (A.1c)). The branching process approximation greatly

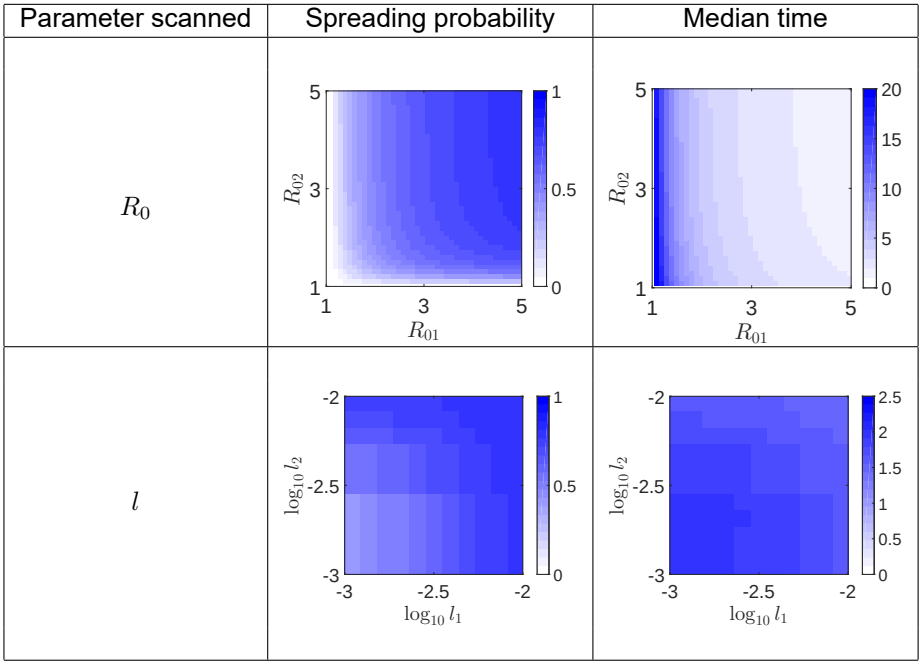

Figure 5: *For a wide range of parameter values, decreasing R_0 in either patch or decreasing l in each patch decreases the spreading probability and delays the median spreading time; however, decreasing R_0 in the first patch is the most effective way of doing so.* The effect of changing (top) R_{01} and R_{02} or (bottom) l_1 and l_2 on (left) the spreading probability and (right) the median spreading time conditioning on this occurring, calculated using approximation (1b) in Section 2.3. All other parameter values are as per Table 1. Note that the two figures on the right have different scales because they encompass different ranges of values.

reduces computing time. Using deterministic or hybrid disease dynamics further drops the computing time from $\mathcal{O}(N_{L1} + N_{T1})$ to $\mathcal{O}(1)$. As Section 3.1 focuses on parameter changes in the context of interventions, the effect of changing the population size on the spreading time distribution is not included in the main text, but is given in Section 3 of the Supplementary Material.

To check whether computational efficiency comes at the expense of accuracy, we now compare the spreading time distributions obtained using different degrees of approximation. The key result is that depending on the parameters used, the accuracy of the spreading time distribution evaluated using each of the approximations changes.

Figure 7 shows the cumulative density function (left) and the probability density function (right) of the spreading time for different computational methods. For the case where $R_{01} = R_{02} = 5$ (Fig. 7A), the spreading time distrubution is very similar for all methods except for approximation (1a), which overestimates the spreading probability (the cumulative density function approaches a higher value). This overestimation occurs because approximation (1a) assumes that the epidemic becomes established in Patch 1; if this is not

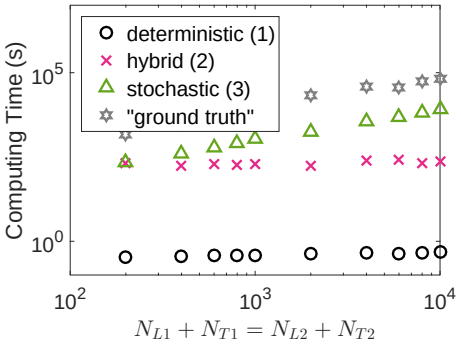

Figure 6: *The branching process approximation increases the computational efficiency of evaluating the spreading time distribution. Efficiency is further gained by assuming either deterministic or hybrid disease dynamics in Patch 1.* The computing time for each of approximations (1)–(3), as well as the 'ground truth', as the population size increases. Note that approximations (1a) and (1b) have the same computing time. The parameters used are those in Table 1. Stochastic/hybrid simulations are run 1000 times.

the case, the number of infectious individuals leaving that patch is much lower, leading to a much lower spreading probability. This discrepancy is of interest because many existing studies of the spreading time distribution (such as that by Barthélemy et al. (2010)) also assume that the epidemic becomes established in Patch 1. Effectively, these studies model the spreading time distribution conditioning on a major outbreak occurring in Patch 1. This conditioning may be appropriate if we are performing risk assessment when the epidemic in Patch 1 is already large, but is not appropriate during early stages when a large outbreak in Patch 1 can still be averted due to stochasticity and/or early interventions.

When $R_{01} = 1.1$ and $R_{02} = 5$ (Fig. 7B), results are approximation-dependent. In this case, approximation (1a) still overestimates the spreading probability, but scaling (approximation (1b)) over-corrects for this. The underestimation occurs because approximation (1b) ignores the possibility that a major outbreak occurs in Patch 2 despite one not occurring in Patch 1. This scenario is relatively more likely when R_{01} is small. Moreover, the median spreading time is overestimated. Section 2.2 in the Supplementary Material analyses this phenomenon in more detail.

In the Supplementary Material, the discrepancies between the approximations and the 'ground truth' model are explored for a wider range of parameter values. Section 1 shows that despite quantitative discrepancies, the qualitative effects of interventions are the same regardless of the approximations used. The relative effectiveness of interventions is also qualitatively the same regardless of the approximations used, with the exception of approximation (1a), which incorrectly predicts that reducing R_0 in either patch is equally effective at reducing the spreading probability. Section 2 analyses the quantitiative discrepancies introduced by the branching process approximation (Section 2.1) and by using deterministic/hybrid disease dynamics (Section 2.2).

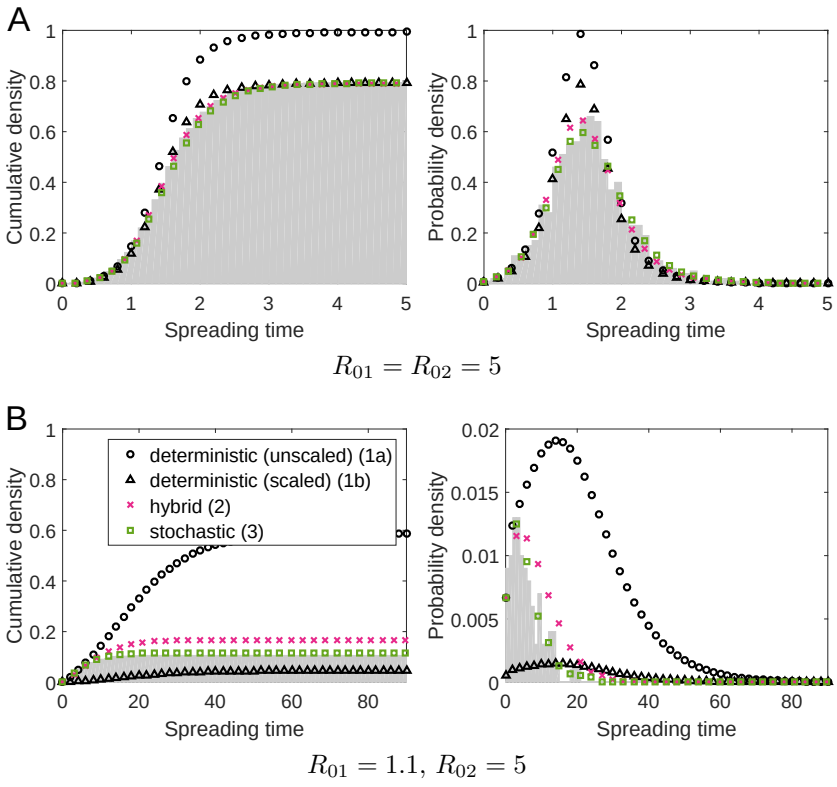

Figure 7: *Approximation (1a) overestimates the spreading probability. The effects of other approximations are parameter-dependent.* The cumulative density function (left) and probability density function (right) of the spreading time for different computational methods. The grey area shows the 'ground truth' model, while markers indicate approximations (1-3), which all use the branching process approximation but with deterministic, hybrid, or stochastic wiithin-patch disease dynamics. The values of R_0 are indicated under each subfigure. The other parameter values are listed in Table 1. For approximations (2-3), we use bootstrapping to obtain estimates of the distribution at a given spreading time; we plot the median of the bootstrap samples. Note the different scales between the probability density functions. The distributions are improper; the area under the curve represents the spreading probability.

4. Conclusion

In this study, we have modelled disease spread between two regions. We constructed a branching process in Patch 2 and combined it with epidemic trajectories in Patch 1 to derive equations for the spreading probability and spreading time distribution. This approach decouples the contributions to the spreading time distribution by travel parameters and disease parameters in Patch 2, and by disease parameters in Patch 1. Previous studies (such as by Lahodny & Allen (2013)) have used the branching process approximation to evaluate the probability that the epidemic undergoes early extinction in all populations, but a branching process across both patches is not appropriate for evaluating the spreading probability (Milliken, 2017).

We used this model to show that decreasing the outbreak size in Patch 1 through decreasing R_{01} is more effective at either preventing or delaying an outbreak in Patch 2, compared to decreasing R_{02} or reducing travel. These qualitative effects are the same regardless of the approximations used, and the branching process approximation is more computationally efficient, especially when used with deterministic or hybrid disease dynamics in Patch 1. However, quantitative differences between spreading time distributions evaluated using different approximations are parameter-dependent. Importantly, if deterministic disease dynamics are assumed in Patch 1, the probability density function must be scaled to account for the possibility that a major outbreak does not occur in Patch 1; otherwise, the spreading probability is overestimated, and the effectiveness of reducing R_{01} is underestimated. Previous studies have not accounted for possible early epidemic fadeout in the source patch when evaluating the spreading time. Wang & Wu (2018) conjectured that when using deterministic disease dynamics, stochastic effects could be accounted for by simply multiplying the probability of each importion event by the outbreak probability, which in our case is the outbreak probability for the branching process. This approach considers epidemic fadeout in the second patch to be the only effect of stochastic transmission dynamics. In our study, we have also incorporated the effects of epidemic fadeout in the source patch, as previously discussed, and the effects of stochasticity in the epidemic trajectories in Patch 1. We have identified regions of parameter space where stochasticity greatly affects the epidemic trajectories in Patch 1, in turn affecting the spreading time distribution. Hence, the conjecture by Wang & Wu (2018) is only partially accurate in these regions; instead of simply multiplying the importation probability by a factor, stochastic epidemic trajectories in Patch 1 should be used.

A limitation of this study is the assumption that model parameters are known and the effects of the intervention on disease and travel parameters can be quantified. However, R_0 is difficult to estimate during the early stages of the epidemic, for example because of inhomogeneous mixing or observation biases (Nishiura et al., 2010; Mercer et al., 2011; Chowell et al., 2016; Rebuli et al., 2018). Furthermore, the disease parameters for the patches to which the epidemic has yet to spread are unknown, and quantifying the rate of short trips between patches requires extensive data collection. Of course, this limitation

applies to all methods for predicting the spreading time. Nevertheless, because we can now efficiently calculate the spreading time distribution, the effects of interventions can be explored over a range of biologically plausible parameters.

We envisage a number of possible extensions to this work.

First, one can examine different network structures connecting more than two patches. The more straightforward case is determining the spreading time from an initial patch to any second patch (rather than the spreading time to a specific patch). Determining the spreading time to a specific patch is difficult because of multiple possible routes of disease spread through the network to that patch. For a star network, which avoids this difficulty, it has been shown that decreasing the reproduction number in the central patch has the greatest effect on reducing the epidemic final size (Arino, 2017). However, the effects of interventions on the spreading time were not examined in the study; moreover, the deterministic model used does not capture the possibility that an intervention could prevent disease spread altogether.

For our two-patch model, to determine the spreading time we only need to simulate epidemic trajectories within Patch 1. For a model with more patches, a further difficulty is that once infection spreads beyond Patch 1, continued movement of individuals between infected patches may change the epidemic trajectories within each infected patch, and thus change the spreading time to further uninfected patches. Thus, a metapopulation model may be required to simulate epidemic trajectories within infected patches. Previous studies have estimated the spreading times for various networks of patches (Swinton, 1998; Park et al., 2002; Gautreau et al., 2008; Wang & Wu, 2018) and calculated the distribution of the final number of infected patches (Ball et al., 1997; Colizza & Vespignani, 2007; Barthélemy et al., 2010). However, these studies have either assumed exponential epidemic growth within each patch, or assumed that beyond the initial seeding event, epidemics within each patch are unaffected by between-patch movement.

Second, the spreading time distribution for different within-patch disease dynamics models can be calculated using the general approach in this study: simulating disease dynamics within Patch 1, then calculating the probability that each import from each compartment causes a major outbreak in Patch 2. For example, for the SEIR model, a major outbreak can be caused by importation of either an exposed or an infectious individual. The case where permanent migration is assumed has been previously studied (Wang & Wu, 2018). In this case, exposed imported individuals are guaranteed to become infectious in Patch 2; then, the probabilities of a major outbreak given one importation are the same for an exposed and an infectious individual. However, if temporary travel is assumed, an exposed traveller in Patch 2 may return to their home patch before becoming infectious. Then, the probabilities of a major outbreak given importation are different for exposed and infectious individuals, so the equations to be solved for the spreading probability per import (corresponding to Eq. 8) will be different for the SEIR and SIR models.

For each within-patch model, the assumptions required to convert a 'ground truth' model into a reduced model will be different, so extensive sensitivity

analysis will be needed to assess accuracy losses. Hence, this extension is the subject of future work. However, to intuit what may change for a more complicated model, we can use the breakdown of the calculation into simulating disease dynamics within Patch 1, then calculating the spreading probability per import. For example, for the SEIR model, compared to the SIR model with the same values of β_i and γ_i, the final size distribution is approximately the same (it is the same for a single-patch model). Thus, the distribution of the area under the prevalence curve for the number of infectious individuals, and hence this term's contribution to the spreading time, is the same. However, there is an additional contribution due to the importation of exposed individuals. Hence, we expect the spreading probability to be greater for the SEIR model. However, the slower time course of the epidemic in Patch 1 for the SEIR model suggests that conditional on the epidemic spreading, the median spreading time will be slower.

Third, to better reflect social structure, the assumption that each compartment travels at the same rate can be relaxed. For example, one could have a subpopulation which never travels, and a regularly travelling subpopulation. This modification would increase the probability that an infectious traveller travels multiple times, which is negligible in our model.

Fourth, one can identify the conditions under which modelling travel as temporary predicts a different spreading time distribution to modelling travel as permanent migration. This information will tell us when data on travel duration is required.

Last, the modelling of interventions can be refined In our study, interventions take immediate effect upon disease introduction in Patch 1, but in reality, delays may decrease their effectiveness. For example, if the time to vaccination rollout is long, then vaccination in the source patch may not be able to conrol the outbreak there, and pre-emptively vaccinating neighbouring patches becomes relatively more effective (Kelly Jr. et al., 2016).

The relationships between the spreading time distribution and other quantities of interest, such as the number of seeding events, the extinction time, and the final size, remain open questions. For example, the extinction time and final size distributions for a two-patch model have been explored numerically (Hernandez-Ceron et al., 2015), but the dependence of these distributions on the spreading time is unknown. It is also unclear how ongoing travel after the initial seeding event modifies the extinction time and final size of the outbreak in each patch. A better understanding of these quantities will guide intervention assessment.

Acknowledgements

A. W. C. Y. was supported by an ACS Foundation Scholarship and an Australian Postgraduate Award (now Australian Government Research Training Program Scholarship). A. J. B. was supported by an Australian Research Council Discovery Early Career Researcher Award (DE160100690). J. V. R. is supported by an Australian Research Council Future Fellowship (FT130100254).

A. W. C. Y., J. M. M. and J. V. R. are supported by the National Health and Medical Research Centre of Australia Centre for Research Excellence Policy Relevant Infectious disease Simulation and Mathematical Modelling (PRISM^2; 1078068).

Arino, J. (2017). Spatio-temporal spread of infectious pathogens of humans. *Infectious Disease Modelling*, *2*, 218 – 228. doi:10.1016/j.idm.2017.05.001.

Balcan, D., & Vespignani, A. (2012). Invasion threshold in structured populations with recurrent mobility patterns. *Journal of Theoretical Biology*, *293*, 87 – 100. doi:10.1016/j.jtbi.2011.10.010.

Ball, F. (1983). The threshold behaviour of epidemic models. *Journal of Applied Probability*, *20*, 227–241.

Ball, F., Mollison, D., & Scalia-Tomba, G. (1997). Epidemics with two levels of mixing. *The Annals of Applied Probability*, *7*, pp. 46–89.

Ballard, P., Bean, N., & Ross, J. (2016). The probability of epidemic fadeout is non-monotonic in transmission rate for the Markovian SIR model with demography. *Journal of Theoretical Biology*, *393*, 170 – 178. doi:https://doi.org/10.1016/j.jtbi.2016.01.012.

Barbour, A. D. (1974). On a functional central limit theorem for Markov population processes. *Advances in Applied Probability*, *6*, 21–39.

Barthélemy, M., Godrèche, C., & Luck, J.-M. (2010). Fluctuation effects in metapopulation models: Percolation and pandemic threshold. *Journal of Theoretical Biology*, *267*, 554 – 564. doi:10.1016/j.jtbi.2010.09.015.

Chowell, G., Viboud, C., Simonsen, L., & Moghadas, S. M. (2016). Characterizing the reproduction number of epidemics with early subexponential growth dynamics. *Journal of The Royal Society Interface*, *13*. doi:10.1098/rsif.2016.0659.

Cliff, A., Smallman-Raynor, M., Haggett, P., Stroup, D., Thacker, S. et al. (2009). *Emergence and re-emergence. Infectious diseases: a geographical analysis*. Oxford University Press.

Colizza, V., & Vespignani, A. (2007). Invasion threshold in heterogeneous metapopulation networks. *Physical Review Letters*, *99*, 148701. doi:10.1103/PhysRevLett.99.148701.

Eaton, J. W., Bateman, D., Hauberg, S., & Wehbring, R. (2015). *GNU Octave version 4.0.0 manual: a high-level interactive language for numerical computations*. URL: http://www.gnu.org/software/octave/doc/interpreter.

Gautreau, A., Barrat, A., & Barthélemy, M. (2008). Global disease spread: Statistics and estimation of arrival times. *Journal of Theoretical Biology*, *251*, 509 – 522. doi:10.1016/j.jtbi.2007.12.001.

Gillespie, D. T. (1977). Exact stochastic simulation of coupled chemical reactions. *The Journal of Physical Chemistry*, *81*, 2340–2361. doi:10.1021/j100540a008.

Harris, T. E. (1963). *The Theory of Branching Processes*. (1st ed.). The RAND Corporation.

Hernandez-Ceron, N., Chavez-Casillas, J. A., & Feng, Z. (2015). Discrete stochastic metapopulation model with arbitrarily distributed infectious period. *Mathematical Biosciences*, *261*, 74 – 82. doi:10.1016/j.mbs.2014.12.003.

Jenkinson, G., & Goutsias, J. (2012). Numerical integration of the master equation in some models of stochastic epidemiology. *PLoS ONE*, *7*, 1–9. doi:10.1371/journal.pone.0036160.

Keeling, M. J., & Rohani, P. (2002). Estimating spatial coupling in epidemiological systems: a mechanistic approach. *Ecology Letters*, *5*, 20–29. doi:10.1046/j.1461-0248.2002.00268.x.

Kelly Jr., M. R., Tien, J. H., Eisenberg, M. C., & Lenhart, S. (2016). The impact of spatial arrangements on epidemic disease dynamics and intervention strategies. *Journal of Biological Dynamics*, *10*, 222–249. doi:10.1080/17513758.2016.1156172.

Kimmel, M., & Axelrod, D. E. (2015). *Branching Processes in Biology*. Springer, New York, NY.

Kurtz, T. G. (1970). Solutions of ordinary differential equations as limits of pure jump Markov processes. *Journal of Applied Probability*, *7*, 49–58.

Kurtz, T. G. (1971). Limit theorems for sequences of jump Markov processes approximating ordinary differential processes. *Journal of Applied Probability*, *8*, 344–356.

Lahodny, G. E., & Allen, L. J. S. (2013). Probability of a disease outbreak in stochastic multipatch epidemic models. *Bulletin of Mathematical Biology*, *75*, 1157–1180. doi:10.1007/s11538-013-9848-z.

Lopez, L. F., Amaku, M., Coutinho, F. A. B., Quam, M., Burattini, M. N., Struchiner, C. J., Wilder-Smith, A., & Massad, E. (2016). Modeling importations and exportations of infectious diseases via travelers. *Bulletin of Mathematical Biology*, *78*, 185–209. doi:10.1007/s11538-015-0135-z.

MATLAB (2015). *R2015b*. Natick, Massachusetts: The MathWorks Inc.

Mercer, G. N., Glass, K., & Becker, N. G. (2011). Effective reproduction numbers are commonly overestimated early in a disease outbreak. *Statistics in Medicine*, *30*, 984–994. doi:10.1002/sim.4174.

Milliken, E. (2017). The probability of extinction of infectious salmon anemia virus in one and two patches. *Bulletin of Mathematical Biology*, *79*, 2887–2904. doi:10.1007/s11538-017-0355-5.

Nishiura, H., Chowell, G., Safan, M., & Castillo-Chavez, C. (2010). Pros and cons of estimating the reproduction number from early epidemic growth rate of influenza A (H1N1) 2009. *Theoretical Biology and Medical Modelling*, *7*, 1. doi:10.1186/1742-4682-7-1.

Park, A. W., Gubbins, S., & Gilligan, C. A. (2002). Extinction times for closed epidemics: the effects of host spatial structure. *Ecology Letters*, *5*, 747–755. doi:10.1046/j.1461-0248.2002.00378.x.

Rebuli, N. P., Bean, N. G., & Ross, J. V. (2016). Hybrid Markov chain models of S–I–R disease dynamics. *Journal of Mathematical Biology*, *75*, 521–541. doi:10.1007/s00285-016-1085-2.

Rebuli, N. P., Bean, N. G., & Ross, J. V. (2018). Estimating the basic reproductive number during the early stages of an emerging epidemic. *Theoretical Population Biology*, *119*, 26 – 36. doi:https://doi.org/10.1016/j.tpb.2017.10.004.

Rvachev, L. A., & Longini, I. M. (1985). A mathematical model for the global spread of influenza. *Mathematical Biosciences*, *75*, 3–22. doi:10.1016/0025-5564(85)90064-1.

Swinton, J. (1998). Extinction times and phase transitions for spatially structured closed epidemics. *Bulletin of Mathematical Biology*, *60*, 215–230. doi:10.1006/bulm.1997.0014.

Wang, L., & Wu, J. T. (2018). Characterizing the dynamics underlying global spread of epidemics. *Nature Communications*, *9*, 218. doi:10.1038/s41467-017-02344-z.

Appendix A. Formal definitions of the continuous-time Markov chain models

The model in Fig. 1 can be specified as a continuous-time Markov chain (CTMC) $\{\mathbf{X}(t)\}_{t\geq 0}$ which takes values $(S_{L1}, I_{L1}, R_{L1}, S_{T2}, I_{T2}, S_{L2}, I_{L2}, R_{L2}, S_{T1}, I_{T1})$ from the ten-dimensional lattice

$$\chi = \{(S_{L1}, I_{L1}, R_{L1}, S_{T2}, I_{T2}, S_{L2}, I_{L2}, R_{L2}, S_{T1}, I_{T1}) \in \mathbb{Z}_+^{10} : \tag{A.1a}$$

$$S_{L1} + I_{L1} + R_{L1} + S_{T2} + I_{T2} \leq N_{L1}(0) + N_{T2}(0), \tag{A.1b}$$

$$S_{L2} + I_{L2} + R_{L2} + S_{T1} + I_{T1} \leq N_{L2}(0) + N_{T1}(0)\}. \tag{A.1c}$$

(R_{T1} and R_{T2} are redundant due to the conservation of the number of individuals local to each patch.) Let $\mathbf{e}_j$ denote the stochiometries (jumps) of $\{\mathbf{X}(t)\}$

j	$\mathbf{e}_j$	$q_X(\mathbf{x}, \mathbf{x}+\mathbf{e}_j)$
1	$(-1,1,0,0,0,0,0,0,0,0)$	$\beta_1 S_{L1} \frac{I_{L1}+I_{T1}}{N_{L1}+N_{T1}}$
2	$(0,0,0,0,0,0,0,0,-1,1)$	$\beta_1 S_{T1} \frac{I_{L1}+I_{T1}}{N_{L1}+N_{T1}}$
3	$(0,0,0,0,0,-1,1,0,0,0)$	$\beta_1 S_{L2} \frac{I_{L2}+I_{T2}}{N_{L2}+N_{T2}}$
4	$(0,0,0,-1,1,0,0,0,0,0)$	$\beta_1 S_{T2} \frac{I_{L2}+I_{T2}}{N_{L2}+N_{T2}}$
5	$(0,-1,1,0,0,0,0,0,0,0)$	$\gamma_1 I_{L1}$
6	$(0,0,0,0,0,0,0,0,0,-1)$	$\gamma_1 I_{T1}$
7	$(0,0,0,0,0,0,-1,1,0,0)$	$\gamma_2 I_{L2}$
8	$(0,0,0,0,-1,0,0,0,0,0)$	$\gamma_2 I_{T2}$
9	$(-1,0,0,1,0,0,0,0,0,0)$	$l_1 S_{L1}$
10	$(0,-1,0,0,1,0,0,0,0,0)$	$l_1 I_{L1}$
11	$(0,0,-1,0,0,0,0,0,0,0)$	$l_1 R_{L1}$
12	$(0,0,0,0,0,-1,0,0,1,0)$	$l_2 S_{L2}$
13	$(0,0,0,0,0,0,-1,0,0,1)$	$l_2 I_{L2}$
14	$(0,0,0,0,0,0,0,-1,0,0)$	$l_2 R_{L2}$
15	$(0,0,0,0,0,1,0,0,-1,0)$	$r_1 S_{T1}$
16	$(0,0,0,0,0,0,1,0,0,-1)$	$r_1 I_{T1}$
17	$(0,0,0,0,0,0,0,1,0,0)$	$r_1 R_{T1}$
18	$(1,0,0,-1,0,0,0,0,0,0)$	$r_2 S_{T2}$
19	$(0,1,0,0,-1,0,0,0,0,0)$	$r_2 I_{T2}$
20	$(0,0,1,0,0,0,0,0,0,0)$	$r_2 R_{T2}$

Table A.3: *Stoichiometries and transition rates of the CTMC* $\{\mathbf{X}(t) = (S_{L1}, I_{L1}, R_{L1}, S_{T2}, I_{T2}, S_{L2}, I_{L2}, R_{L2}, S_{T1}, I_{T1})\}$. R_{T1} and R_{T2} are implicitly tracked by the relations $R_{T1} = N_{L2}(0) + N_{T1}(0) - N_{L2} - S_{T1} - I_{T1}$ and $R_{T2} = N_{L1}(0) + N_{T2}(0) - N_{L1} - S_{T2} - I_{T2}$.

j	$\mathbf{d}_j$	$q_Y(\mathbf{y}, \mathbf{y}+\mathbf{d}_j)$
1	$(-1,1,0,0,0)$	$\beta_1 S_{L1} \frac{I_{L1}+I_{T1}}{N_{L1}+N_{T1}}$
2	$(0,-1,0,0,0)$	$[\gamma_1 + l_1(1-\phi_{T2})]I_{L1}$
3	$(0,-1,0,0,1)$	$l_1\phi_{T2}I_{L1}$
4	$(0,0,-1,1,0)$	$\beta_1 S_{T1} \frac{I_{L1}+I_{T1}}{N_{L1}+N_{T1}}$
5	$(0,0,0,-1,0)$	$[\gamma_1 + r_1(1-\phi_{L2})I_{T1}]$
6	$(0,0,0,-1,1)$	$r_1\phi_{L2}I_{T1}$

Table A.4: *Stoichiometries and transition rates of the CTMC* $\{\mathbf{Y}(t)\} = (S_{L1}, I_{L1}, S_{T1}, I_{T1}, K)$.

and $q_X(\mathbf{x}, \mathbf{x}+\mathbf{e}_j)$ denote the transition rate from $\mathbf{x}$ to $\mathbf{x}+\mathbf{e}_j$, for $j = 1, ..., 12$. The values of $\mathbf{e}_j$ and $q_X(\mathbf{x}, \mathbf{x}+\mathbf{e}_j)$ for all $\mathbf{x} \in \chi$ are given in Table A.3.

The process in Fig. 2 can be modelled using the CTMC $\{\mathbf{Y}(t)\}_{t\geq 0}$ which takes values $(S_{L1}, I_{L1}, S_{T1}, I_{T1}, K)$ from the five-dimensional lattice

$$\Psi = \{(S_{L1}, I_{L1}, S_{T1}, I_{T1}, K) \in \mathbb{Z}_+^3 : S_{L1}+I_{L1} \leq N_{L1}(0)+N_{T2}(0), S_{T1}+I_{T1} \leq N_{L2}(0)+N_{T1}(0), K = 0, 1\} \tag{A.2}$$

where K is a binary variable indicating whether an outbreak has occurred in Patch 2 (whether $\hat{I}$, the number of outbreak-causing infectious individuals, is greater than zero). Let $\mathbf{d}_j$ denote the stochiometries of $\{\mathbf{Y}(t)\}$ and $q_Y(\mathbf{y}, \mathbf{y}+\mathbf{d}_j)$ denote the transition rate from $\mathbf{y}$ to $\mathbf{y}+\mathbf{d}_j$, for $j = 1, \ldots, 5$. The values of $\mathbf{d}_j$ and $q_Y(\mathbf{y}, \mathbf{y}+\mathbf{d}_j)$ for all $\mathbf{y} \in \Psi$ are given in Table A.4.